

# Constraints on the Bulk Lorentz Factor of GRB 990123

Alicia M. Soderberg\* and Enrico Ramirez-Ruiz\*

\**Institute of Astronomy, Madingley Road, Cambridge CB3 0HA, ENGLAND*

**Abstract.** GRB 990123 was a long, complex gamma-ray burst accompanied by an extremely bright optical flash. We present the collective constraints on the bulk Lorentz factor for this burst based on estimates from burst kinematics, synchrotron spectral decay, prompt radio flash observations, and prompt emission pulse width. Combination of these constraints leads to an average bulk Lorentz factor for GRB 990123 of  $\Gamma_0 = 1000 \pm 100$  which implies a baryon loading of  $M_{jet} = 8_{-2}^{+17} \times 10^{-8} M_{\odot}$ . We find these constraints to be consistent with the speculation that the optical light is emission from the reverse shock component of the external shock. In addition, we find the implied value of  $M_{jet}$  to be in accordance with theoretical estimates: the baryonic loading is sufficiently small to allow acceleration of the outflow to  $\Gamma > 100$ .

## INTRODUCTION

The discovery of a prompt and extremely bright optical flash in GRB 990123 (Akerlof et al. 1999), implying an apparent peak (isotropic) optical luminosity of  $5 \times 10^{49} \text{ erg s}^{-1}$ , has led to widespread speculation that the observed radiation arose from the reverse shock component of the burst. The reverse shock propagates into the adiabatically cooled particles of the coasting ejecta, decelerating the shell particles and shocking the shell material with an amount of internal energy comparable to that of the material shocked by the forward shock. The typical temperature in the reverse-shocked fluid is, however, considerably lower than that of the forward-shocked fluid. Consequently, the typical frequency of the synchrotron emission from the reverse shock peaks at lower energy. It is believed to account for the bright prompt optical emission from GRB 990123. The reverse shock emission stops once the entire shell has been shocked and the reverse shock reaches the inner edge of the fluid. Unlike the continuous forward shock, the hydrodynamic evolution of the reverse-shocked ejecta is more fragile. As we will demonstrate, the temperature of the reverse-shocked fluid is expected to be mildly-relativistic for GRB 990123 and thus the evolution of the ejecta deviates from the Blandford & McKee (BM) solution that determines the late profile of the decelerating shell and the external medium. In general, the determination of  $\Gamma_0$  for optical flashes, would play an important role in discriminating between *cold* and *hot* shell evolution. Moreover, the strong dependence of the peak time of the optical flash on the bulk Lorentz factor  $\Gamma$  provides a way to estimate this elusive parameter. We discuss how

different constraints on  $\Gamma_0$  for GRB 990123 are consistent with optical emission from the reverse shock. We assume  $H_0 = 65 \text{ km s}^{-1} \text{ Mpc}^{-1}$ ,  $\Omega_M = 0.3$ , and  $\Omega_{\Lambda} = 0.7$ .

## THE ROLE OF $\Gamma$

Relativistic source expansion plays a crucial role in virtually all current GRB models (Piran 1999; Mészáros 2001). The Lorentz factor is not, however, well determined by observations. The lack of apparent photon-photon attenuation up to  $\approx 0.1 \text{ GeV}$  implies only a lower limit  $\Gamma \approx 30$  (Mészáros, Laguna & Rees 1993), while the observed pulse width evolution in the gamma-ray phase eliminates scenarios in which  $\Gamma \gg 10^3$  (Lazzati, Ghisellini & Celotti 2001; Ramirez-Ruiz & Fenimore 2000). The initial Lorentz factor is set by the baryon loading, that is  $m_0 c^2$ , where  $m_0$  is the mass of the expanding ejecta. This energy must be converted to radiation in an optically-thin region, as the observed bursts are non-thermal. The radius of transparency of the ejecta is

$$R_{\tau} = \left( \frac{\sigma_T E}{4\pi m_p c^2 \Gamma_0} \right)^{1/2} \approx 10^{12} - 10^{13} \text{ cm}, \quad (1)$$

where  $E$  is the isotropic equivalent energy generated by the central site. The highly variable  $\gamma$ -ray light curves can be understood in terms of internal shocks produced by velocity variations within the relativistic outflow (Rees & Mészáros 1994). In an unsteady outflow, if  $\Gamma$  were to vary by a factor of  $\approx 2$  on a timescale  $\delta T$ , then internal shocks would develop at a distance  $R_i \approx \Gamma^2 c \delta T \geq R_{\tau}$ . This is followed by the development of a blast wave

expanding into the external medium, and a reverse shock moving back into the ejecta. The inertia of the swept-up external matter decelerates the shell ejecta significantly by the time it reaches the deceleration radius (Mészáros & Rees 1993),

$$R_d = \left( \frac{E}{n_0 m_p c^2 \Gamma_0^2} \right)^{1/3} \approx 10^{16} - 10^{17} \text{ cm.} \quad (2)$$

Given a certain external baryon density  $n_0$ , the initial Lorentz factor then strongly determines where both internal and external shocks develop. Changes in  $\Gamma_0$  will modify the dynamics of the shock deceleration and the manifestations of the afterglow emission.

## REVERSE SHOCK EMISSION AND $\Gamma_0$

It has been predicted that the reverse shock produces a prompt optical flash brighter than 15th magnitude with reasonable energy requirements of no more than a few  $10^{53}$  erg emitted isotropically (Mészáros & Rees 1999; Sari & Piran 1999a; hereinafter MR99 and SP99). The forward shock emission is continuous, but the reverse shock terminates once the shock has crossed the shell and the cooling frequency has dropped below the observed range. The reverse shock contains, at the time it crosses the shell, an amount of energy comparable to that in the forward one. However, its effective temperature is significantly lower (typically by a factor of  $\Gamma$ ). Using the shock jump conditions and assuming that the electrons and the magnetic field acquire a fraction of the equipartition energy  $\epsilon_e$  and  $\epsilon_B$  respectively, one can describe the hydrodynamic and magnetic conditions behind the shock.

The reverse shock synchrotron spectrum is determined by the ordering of three break frequencies, the self-absorption frequency  $\nu_a$ , the cooling frequency  $\nu_c$  and the characteristic synchrotron frequency  $\nu_m$ , which are easily calculated by comparing them to those of the forward shock (MR99; SP99; Panaitescu & Kumar 2000). The equality of energy density across the contact discontinuity suggests that the magnetic fields in both regions are of comparable strength.

Assuming that the forward and reverse shocks both move with a similar Lorentz factor, the reverse shock synchrotron frequency is given by

$$\nu_m = 5.840 \times 10^{13} \epsilon_{e,-1}^2 \epsilon_{B,-2}^{1/2} n_{0,0}^{1/2} \Gamma_{0,2}^2 (1+z)^{-1/4} \text{ Hz,} \quad (3)$$

while the cooling frequency  $\nu_c$  is equal to that of the forward shock. Here we adopt the convention  $Q = 10^x Q_x$  for expressing the physical parameters, using cgs units. The spectral power  $F_{\nu_m}$  at the characteristic synchrotron frequency is

$$F_{\nu_m} = 4.17 D_{28}^{-2} \epsilon_{B,-2}^{1/2} E_{53} n_{0,0}^{1/2} \Gamma_{0,2} (1+z)^{3/8} \text{ Jy.} \quad (4)$$

The distribution of the injected electrons is assumed to be a power law of index  $-p$ , above a minimum Lorentz factor  $\gamma_i$ . For an adiabatic blast wave, the corresponding spectral flux at a given frequency above  $\nu_m$  is  $F_\nu \approx F_{\nu_m} (\nu/\nu_m)^{-(p-1)/2}$ , while below  $\nu_m$  is characterised by a synchrotron tail with  $F_\nu \approx F_{\nu_m} (\nu/\nu_m)^{1/3}$ . Similar relations to those found for a radiative forward shock hold for the reverse shock (Kobayashi 2000; hereinafter K00).

Unlike the synchrotron spectrum, the afterglow light curve at a fixed frequency strongly depends on the hydrodynamics of the relativistic shell, which determines the temporal evolution of the break frequencies  $\nu_m$  and  $\nu_c$ . The forward shock is always highly relativistic and thus is successfully described using the relativistic generalisation of theory of supernova remnants. In contrast, the reverse shock can be mildly relativistic. In this regime, the shocked shell is unable to heat the ejecta to sufficiently high temperatures and its evolution deviates from the BM solution (Kobayashi & Sari 2000; hereinafter KS00). Shells satisfying

$$\xi \approx 0.01 E_{52}^{1/6} \Delta_{11}^{-1/2} \Gamma_{0,2}^{-4/3} n_{0,1}^{-1/6} > 1, \quad (5)$$

are likely to have a Newtonian reverse shock<sup>1</sup>, otherwise the reverse shock is relativistic and it considerably decelerates the ejecta. The width of the shell,  $\Delta$ , can be inferred directly from the observed burst duration by  $\Delta = c T_{\text{dur}} / (1+z)$  assuming the shell does not undergo significant spreading (Piran 1999).

If  $\xi > 1$ , then the reverse shock is in the sub-relativistic temperature regime for which there are no known analytical solutions. In order to constrain the evolution of  $\Gamma$  in this regime it is common to assume  $\Gamma \propto R^{-g}$  where  $3/2 \leq g \leq 7/2$  (MR99; KS00). For an adiabatic expansion,  $\Gamma \propto T^{-g/(1+2g)}$  and so  $\nu_m \propto T^{-3(8+5g)/7(1+2g)}$  and  $F_{\nu_m} \propto T^{-(12+11g)/7(1+2g)}$ . The spectral flux at a given frequency expected from the reverse shock gas drops then as  $T^{-2(2+3g)/7(1+2g)}$  below  $\nu_m$  and  $T^{-(7+24p+15pg)/14(1+2g)}$  above. For a typical spectral index  $p = 2.5$ , the flux decay index varies in a relatively narrow range ( $\approx 0.4$ ) between limiting values of  $g$ .

## CONSTRAINTS ON THE $\Gamma_0$ OF GRB 990123

Despite ongoing observational attempts, the optical flash associated with GRB 990123 remains the only event of its kind detected to date. Observations of this optical

<sup>1</sup> It should be remarked that equations (3) and (4) refer to this reverse shock regime. Equations for the relativistic case are relatively similar, the biggest discrepancy being that the peak flux is inversely proportional to  $\Gamma$  (see equations (7)-(9) of K00).

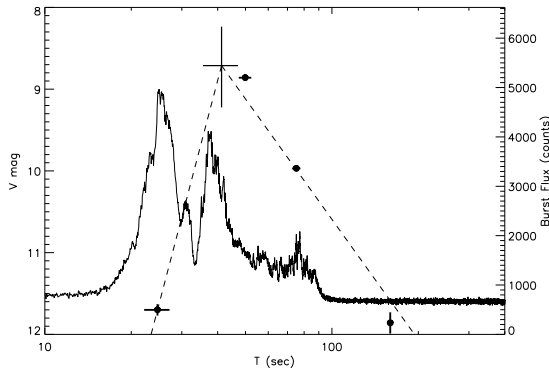


**FIGURE 1.** BATSE and ROTSE light curves for GRB 990123 as a function of time from the BATSE trigger. Dashed lines represent theoretical predictions for the rise  $\propto T^{3p-3/2}$  and decay  $\propto T^{-(21+73p)/96}$  of an adiabatic reverse shock light curve, assuming the shell is thin and cooling slowly. We predict that the optical flash peaked  $\approx 41 \pm 6$  seconds after the trigger.

flash appear to be in good agreement with early predictions for the reverse shock emission (Sari & Piran 1999b). As a result, numerous studies have been done on this event in which reverse shock theory has been applied to burst observations in order to constrain physical parameters and burst properties, including  $\Gamma_0$ . Current estimates on the bulk Lorentz factor for GRB 990123 stretch over nearly an order of magnitude, with values ranging from  $\approx 200$  (SP99) to  $\approx 1200$  (Wang, Dai & Lu 2000). It should be noted, however, that these estimates were made before accurate burst parameters for GRB 990123 were known, and consequently they include approximations and parameters from other GRB afterglows.

By fitting multi-frequency afterglow light curves, physical parameters for 8 GRBs have recently been reported (Panaitescu & Kumar 2001b, hereinafter PK01). Best fit values presented for GRB 990123 are  $E_{j,50} = 1.5_{-0.4}^{+3.3}$  (initial jet energy),  $\theta_0 = 2.1_{-0.9}^{+0.1}$ ,  $n_{0,-3} = 1.9_{-1.5}^{+0.5}$ ,  $\epsilon_{e,-2} = 13_{-4}^{+1}$ ,  $\epsilon_{B,-4} = 7.4_{-5.9}^{+23}$ , and  $p = 2.28_{-0.03}^{+0.05}$  with a rough estimate for the bulk Lorentz factor of  $\Gamma_0 = 1400 \pm 700$  (Panaitescu & Kumar 2001a). Using these physical parameters, we present a comprehensive examination of the constraints on  $\Gamma_0$  and report a best-fit value based on an analysis of these constraints.

*Time of Peak Flux.* Observational estimates for the time of peak flux enabled a measurement of the initial Lorentz factor with reasonable accuracy using the physical parameters specific to GRB 990123. Assuming the optical flash was the result of the reverse shock, the initial bulk Lorentz factor

$$\Gamma_0 = 237 E_{52}^{1/8} n_{0,0}^{-1/8} T_{d,1}^{-3/8} (1+z)^{3/8} \quad (6)$$

where  $T_d$  is the time of peak flux in the observer frame. Light curves for the optical flash and  $\gamma$ -ray emission are shown in Figure 1. Dashed lines represent theoretical predictions for the rise  $\propto T^{3p-3/2}$  and decay  $\propto T^{-(21+73p)/96}$  of an adiabatic reverse shock light curve, assuming the shell is thin, i.e.  $\Delta < (E/(2n_0 m_p c^2 \Gamma_0^8))^{1/3}$ , and cooling slowly (K00). Using the recently reported physical parameters, one finds GRB 990123 to have a marginal thickness, as predicted by K00. The observed rise time is, however, in good agreement with that of a thin shell  $\approx T^{5.5}$  (in contrast with  $\approx T^{1/2}$  for a thick shell). The shape of the light curve is determined by the time evolution of the three spectral break frequencies, which in turn depend on the hydrodynamical evolution of the fireball. In the case of GRB 990123, the typical synchrotron frequency  $\nu_m = 1.5 \times 10^{14}$  Hz is well below the cooling frequency  $\nu_c = 1.0 \times 10^{19}$  Hz, and therefore places the burst in a regime with a flux decay governed by the relation  $F_\nu \propto T^{-(21+73p)/96}$ . This implies a decay of  $\approx T^{-2}$  for the optical flash of GRB 990123. Applying these light curve predictions to the prompt optical data and taking observational uncertainties as well as burst parameter uncertainties into account, we predict that the optical flash peaked  $T_{\text{peak}} \approx 41 \pm 6$  s after the GRB started. Substitution for  $T_{\text{peak}}$  in equation (6) gives  $\Gamma_0 = 770 \pm 50$ .

*Synchrotron Spectral Decay.* Observations of the optical peak brightness enable further accurate constraints on the value of  $\Gamma_0$ . The synchrotron spectrum from relativistic electrons comprises four power-law segments, separated by three critical frequencies. The prompt optical flash in GRB 990123 is observed at a frequency that falls well below the cooling frequency, but above the typical synchrotron frequency:  $\nu_a < \nu_m < \nu_{\text{obs}} < \nu_c$ . The synchrotron spectrum for this spectral segment is given by  $F_{\text{obs}} = F_{\nu_m} (\nu_{\text{obs}}/\nu_m)^{(p-1)/2} (1+z)^{1/2-p/8}$  where  $\nu_{\text{obs}}$  is taken to be the ROTSE optical frequency. Assuming the optical peak flux  $F_{\text{obs}}$  observed in GRB 990123 is radiation arising from the reverse shock, we find  $\Gamma_0 = 1800_{-500}^{+600}$ .

*Radio Flare Observations.* In addition to the optical flash associated with GRB 990123, a short ( $\sim 30$  hr.) radio flare was also observed (Kulkarni et al., 1999). Since the emission did not grow stronger with time thereby demonstrating the properties of a typical radio afterglow, it was subsequently proposed that both the prompt optical emission and the radio flare arose from the reverse shock (SP99). As the reverse shock cools the emission shifts to lower frequencies which rapidly approach the observational radio band. The received flux peaks when  $\nu_m$  crosses the band while decreasing mildly relativistically as  $\nu_m \propto T^{-3(8+5g)/7(1+2g)}$ . At  $t < 1.2$  days after the initial GRB trigger, the radio flare from 990123 was

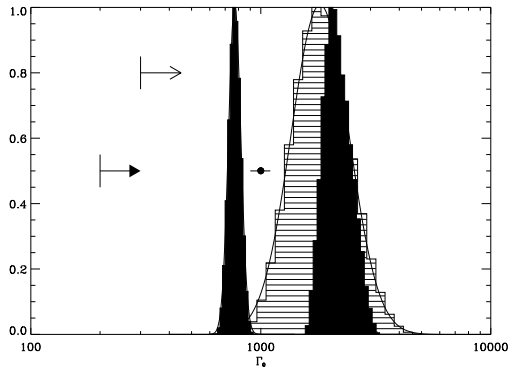


**FIGURE 2.** Collective constraints on  $\Gamma_0$  for GRB 990123. These include estimates from the burst kinematics (narrowest distribution), synchrotron spectral decay (widest distribution), radio flash observations (medium width distribution), prompt emission pulse width (filled arrow), and jet modelling (unfilled arrow). We find a best fit value of  $\Gamma_0 = 1000 \pm 100$ .

observed to be increasing thereby implying  $v_m > v_{\text{obs}}$ . Using eqn (3) and the evolution of  $v_m$ , we compute the  $\Gamma_0$  which places the peak frequency in the radio band at  $t \sim 1.2$  days. We find  $\Gamma_0 = 2000^{+400}_{-200}$ .

*Prompt Emission Pulse Width.* Although observations of a reverse shock induced optical peak enable fairly accurate calculations of the bulk Lorentz factor, it remains possible to obtain information on  $\Gamma_0$  in situations when an optical flash has not been detected. Consider an internal shock which produces an instantaneous burst of isotropic  $\gamma$ -ray emission at a time,  $t$ , and radius,  $R_i$ , in the frame of the central engine. The kinematics of colliding shells implies that although photons are emitted simultaneously, the curvature of the emitting shell spreads the arrival time of the emission over a period of  $\Delta T_p$ , thereby producing the observed width in individual pulses. The delay in arrival time between on-axis photons and those at  $\theta \approx \Gamma^{-1}$  is a function of the radius of emission and the Lorentz factor according to:  $\Delta T_p / (1+z) = R_i / (2c\Gamma^2)$  where  $\Gamma = \Gamma_0$  in the early phase of the expansion (Fenimore, Madras & Nayashin 1996). In order to allow photons to escape,  $R_i$  must be larger than the radius of transparency  $R_\tau$ . This imposes a lower limit on the initial bulk Lorentz factor such that:  $\Gamma_0 > (R_\tau / 2c\Delta T_p)^{1/2} (1+z)^{1/2}$ . We determine  $\Delta T_p$  for GRB 990123 by measuring the average pulse width through autocorrelation methods based on those described in Fenimore, Ramirez-Ruiz & Wu (1999) and find  $\Delta T_p \approx 0.45$  s. Using the burst parameters to estimate  $R_\tau$  from equation (1) and applying the inequality relation defined above, we find a lower limit of  $\Gamma_0 > 200$ . Figure 2 displays the collective constraints on  $\Gamma_0$  for GRB 990123. An additional lower limit of  $\Gamma_0 > 300$  constraint

from afterglow modelling is also included (Panaitescu & Kumar 2002). The combination of these constraints leads to an average bulk Lorentz factor for GRB 990123 of  $\Gamma_0 = 1000 \pm 100$  which implies  $R_\tau \approx 1.3 \times 10^{14}$  and a baryon loading of  $M_{\text{jet}} = 8_{-2}^{+17} \times 10^{-8} M_\odot$ .

## CONCLUSIONS

We have shown that the collective constraints for the bulk Lorentz factor of GRB 990123 are compatible with current reverse shock theory. In addition, our best fit value of  $\Gamma_0 \approx 1000$  provides confirmation of the ultra-relativistic nature of GRBs. The implied values for  $R_\tau$  and  $M_{\text{jet}}$  are in accordance with GRB theory: the radius of transparency is within theoretical estimates and the baryonic loading is sufficiently small to allow acceleration of the outflow to  $\Gamma > 100$ . As we have discussed, the bulk Lorentz factor plays a crucial role throughout all stages of GRB evolution, and therefore the ability to constrain  $\Gamma_0$  provides clues on the nature of gamma-ray bursts.

We thank A. Blain, D. Lazzati, M. J. Rees and E. Rossi for helpful conversations. AMS was supported by the NSF GRFP. ER-R thanks CONACYT, SEP and the ORS for support.

## REFERENCES

- Akerlof C. W. et al., 1999, *Nature*, 398, 400
- Blandford R. D., McKee C. F., 1976, *Phys. Fluids*, 19, 1130 (BM)
- Fenimore E. E., Madras C. D., Nayakshin S., 1996, *ApJ*, 473, 998
- Fenimore E. E., Ramirez-Ruiz E., Wu B., 1999, *ApJ*, 518, L73
- Kobayashi S., 2000, *ApJ*, 545, 807 (K00)
- Kobayashi S., Sari R., 2000, *ApJ*, 542, 819 (KS00)
- Kulkarni S. P. et al., 1999, *ApJ*, 522, L97
- Lazzati D., Ghisellini G., Celotti, A., 2001, *MNRAS*, 309, L13
- Mészáros P., 2001, *Science*, 291, 79
- Mészáros P., Rees M. J., 1993, *ApJ*, 405, 278
- Mészáros P., Laguna P., Rees M. J., 1993, *ApJ*, 415, 181
- Mészáros P., Rees M. J., 1999, *MNRAS*, 306, L39 (MR99)
- Panaitescu A., Kumar P., 2000, *ApJ*, 543, 66
- Panaitescu A., Kumar P., 2001a, *ApJ*, 554, 667
- Panaitescu A., Kumar P., 2001b, *ApJ*, 560, L49 (PK01)
- Panaitescu A., Kumar P., 2002, *ApJ*, submitted (astro-ph/0109124)
- Piran, T., 1999, *Physics Reports*, 314, 575
- Ramirez-Ruiz E., Fenimore E. E., 2000, *ApJ*, 539, 712
- Rees M. J., Mészáros P., 1994, *ApJ*, 430, L93
- Sari R., Piran T., 1999a, *ApJ*, 517, L109 (SP99)
- Sari R., Piran T., 1999b, *ApJ*, 520, 641
- Wang X. Y., Dai Z. G., Lu T., 2000, *MNRAS*, 319, 1159